Kinetics of Intermolecular Cleavage by Hammerhead Ribozymes†

Martha J. Fedor‡ and Olke C. Uhlenbeck*,§

Department of Chemistry and Biochemistry, University of Colorado, Boulder, Colorado 80309-215, and Department of Biochemistry and Molecular Biology, University of Massachusetts Medical Center, 55 Lake Avenue North, Worcester, Massachusetts 01655

Received June 2, 1992; Revised Manuscript Received September 22, 1992

ABSTRACT: The hammerhead catalytic RNA effects cleavage of the phosphodiester backbone of RNA through a transesterification mechanism that generates products with 2′–3′-cyclic phosphate and 5′-hydroxyl termini. A minimal kinetic mechanism for the intermolecular hammerhead cleavage reaction includes substrate binding, cleavage, and product release. Elemental rate constants for these steps were measured with six hammerhead sequences. Changes in substrate length and sequence had little effect on the rate of the cleavage step, but dramatic differences were observed in the substrate dissociation and product release steps that require helix–coil transitions. Rates of substrate binding and product dissociation correlated well with predictions based on the behavior of simple RNA duplexes, but substrate dissociation rates were significantly faster than expected. Ribozyme and substrate alterations that eliminated catalytic activity increased the stability of the hammerhead complex. These results suggest that substrate destabilization may play a role in hammerhead catalysis.

The satellite RNA of Tobacco Ringspot Virus was found to cleave and ligate in vitro, in the absence of protein (Prody et al., 1986; Buzayan et al., 1986). Comparison of sequences near the cleavage site of several self-cleaving plant RNAs led to the identification of a consensus secondary structure termed the "hammerhead" (Keese & Symons, 1987). The hammerhead consists of three helices of variable length and sequence and 11 unpaired nucleotides surrounding the cleavage site. Truncation experiments confirmed that the self-cleaving activity requires only this portion of the RNA molecule (Buzayan et al., 1986; Forster & Symons, 1987), and the hammerhead secondary structure has been confirmed by mutagenesis experiments (Sampson et al., 1987; Sheldon & Symons, 1989; Koizumi et al., 1988b, 1989; Ruffner et al., 1989, 1990) as well as solution structure studies using NMR (Heus et al., 1990; Pease & Wemmer, 1990; Heus & Pardi, 1990; Odai et al., 1990). Although hammerhead sequences are contained within a single RNA molecule in vivo, intermolecular assembly and cleavage can be achieved by dividing the domain into ribozyme and substrate molecules that associate through base pairing (Sampson et al., 1987; Uhlenbeck, 1987; Haseloff & Gerlach, 1988; Ruffner et al., 1989; Koizumi et al., 1988a, 1989; Jeffries & Symons, 1989). Catalytic turnover of intermolecular hammerheads can be achieved by multiple rounds of assembly, cleavage, and product release requiring formation and melting of RNA duplexes. In this sense, the hammerhead reaction resembles RNA-mediated reactions in splicing and translation, such as U1 snRNA binding to upstream splice sites of introns [reviewed in Rosbash and Seraphin (1991)], U4/U6 association in the spliceosome [reviewed in Guthrie and Patterson (1988)], and mRNA binding to ribosomes through Shine–Dalgarno sequences (Gold et al., 1981).

Because hammerhead structure involves base-paired helices, it is likely that a number of features of the kinetic mechanism can be understood in terms of the familiar helix–coil transition of complementary RNAs. Substrate binding requires formation of base pairs between the ribozyme and the substrate. Following cleavage, disruption of the base pairs between the ribozyme and the products permits product release. If substrate binding and product release are simple helix formation and melting reactions, rates for these steps should resemble those determined for short RNA duplexes (Porschke & Eigen, 1971; Craig et al., 1971; Porschke et al., 1973; Ravetch et al., 1974; Breslauer & Bina-Stein, 1977; Nelson & Tinoco, 1982). Deviation in hammerhead kinetics from the behavior expected for simple duplexes might reflect structural or catalytic properties of the domain. Precedence for this approach can be found in the analysis of the kinetic mechanism of the transesterification catalyzed by the *Tetrahymena* group I intron where substrate binding is much tighter than expected for a simple duplex (Herschlag & Cech, 1990). This ultimately led to the identification of a specific tertiary hydrogen bond between a 2′-hydroxyl in the substrate and an adenosine in the catalytic core of the ribozyme (Pyle & Cech, 1991; Pyle et al., 1992). Here we report the use of steady-state and pre-steady-state kinetics to evaluate the kinetic mechanism for six related hammerhead domains that differ in the length and sequence of their helices.

EXPERIMENTAL PROCEDURES

Preparation of RNAs. Ribozyme and substrate RNAs (Figure 1) were synthesized by T7 RNA polymerase transcription of partially duplex synthetic DNA templates (Milligan et al., 1987) and were purified as previously described (Fedor & Uhlenbeck, 1990). The correct 3′-terminal nucleotide was verified for substrate RNAs and for ribozyme 13 by complete digestion of [5′-^{32}P]pCp 3′-end-labeled material (England & Uhlenbeck, 1978) and two-dimensional PEI-cellulose thin-layer chromatography using appropriate standards (Kochino et al., 1980). Substrate RNAs were also sequenced by partial enzymatic cleavage. The remaining RNAs were identified by coelectrophoresis on denaturing gels

† This work was supported by NIH Grant AI 30242 to O.C.U. and by NIH Grant GM 46422 to M.J.F. We thank the Keck Foundation for their generous support of RNA science on the Boulder campus.

* Author to whom correspondence should be addressed.
‡ University of Massachusetts Medical Center.
§ University of Colorado.

0006-2960/92/0431-12042$03.00/0

with characterized markers. For nonradioactive RNAs, concentrations were determined by assuming a residue extinction coefficient at 260 nm of 6.6×10^3 $M^{-1} \cdot cm^{-1}$. For radioactive RNAs, concentrations were determined from specific activities.

In addition to enzymatic synthesis, substrate and product RNAs were synthesized chemically. Ribonucleoside and deoxyribonucleoside phosphoramidites with *tert*-butyldimethylsilyl blocked 2′-hydroxyl groups (Usman et al., 1987) and phenoxyacetyl blocked amino groups of adenine and guanine bases (Schulhof et al., 1987; Chaix et al., 1989) were supplied by American Bionetics. Following deprotection with ethanolic ammonia (Usman et al., 1990) at room temperature for 24 h and tetra-*n*-butylammonium fluoride, synthetic RNAs were desalted by DEAE chromatography as previously described (Fedor & Uhlenbeck, 1990). Product RNAs were generated by ribozyme cleavage of substrates and purified by denaturing gel electrophoresis. The 3′ cleavage product, S13-P2, was also synthesized chemically.

RNAs were labeled by reaction with T4 polynucleotide kinase and [γ-^{32}P]ATP or by incorporation of [α-^{32}P]CTP during in vitro transcription as previously described (Fedor & Uhlenbeck, 1990). 5′-end-labeled RNA was purified from unlabeled RNA by gel electrophoresis so that the specific activity was the same as that of the [γ-^{32}P]ATP, which was 3000 Ci/mmol. The specific activity of RNA labeled during in vitro transcription was calculated from the specific activity of [α-^{32}P]CTP in the transcription reaction and the number of cytosine residues in the RNA and ranged from 24 to 48 Ci/mmol.

Substrates and products prepared by chemical synthesis produced data that varied less than 2-fold relative to data obtained with RNAs prepared by in vitro transcription in both kinetics and equilibrium binding experiments. With the exception of the experiment reported in Figure 5B, which was carried out with substrate labeled during in vitro transcription and product generated by ribozyme cleavage of a substrate transcribed in vitro, all data reported in this paper are from experiments with chemically synthesized substrates and products.

Kinetics. Multiple turnover reactions were carried out as previously described in 50 mM Tris-HCl, pH 7.5, and 10 mM $MgCl_2$ at 25 °C (Fedor & Uhlenbeck, 1990). In order to disrupt RNA aggregates that can form during storage (Groebe & Uhlenbeck, 1988), separate solutions of ribozyme and substrate RNAs were heated in 50 mM Tris-HCl, pH 7.5, at 95 °C for 1 min and allowed to cool to 25 °C. Each RNA solution was adjusted to a final concentration of 10 mM $MgCl_2$ and allowed to incubate at 25 °C for 15 min. Preincubation in $MgCl_2$ was found necessary to prevent anomalous initial rates that might result from slow adoption of Mg-dependent structures (Fedor & Uhlenbeck, 1990). Cleavage reactions were initiated by combining the ribozyme and the substrate. Samples were removed at intervals, quenched with 8 M urea/25 mM EDTA/0.02% bromophenol blue/0.02% xylene cyanol, and then fractionated by electrophoresis using 20% acrylamide/7 M urea gels. Radioactivity in substrate and product bands was quantitated using a Molecular Dynamics radioanalytic scanner or by scintillation counting of excised bands.

Single-turnover cleavage rates were measured with an excess of ribozyme and a trace amount of 5′-^{32}P-end-labeled substrate. Cleavage rates were first order through the first three half-lives of the reaction, and doubling the amount of substrate had no effect on cleavage rates, verifying that the amount of substrate was very low with respect to ribozyme concentrations. The amount of substrate cleaved by the end of the reaction varied between 70% and 95%. Reaction rates were obtained from the slope of semilogarithmic plots of the amount of substrate (S), normalized to the final extent of cleavage, versus time.

Rates of substrate dissociation (k_{-1}, Figure 2) were measured using partitioning experiments (Rose et al., 1974). Separate solutions of ribozyme, a small amount of [5′-^{32}P]substrate RNA, and nonradioactive substrate or product RNA were heated to 95 °C in 50 mM Tris-HCl, pH 7.5, and preincubated at 25 °C in 10 mM $MgCl_2$ as described above. For a typical experiment, 2 μL of ribozyme was combined with 1 μL of [5′-^{32}P]substrate. Ribozyme concentrations ranged from 20 to 160 times the K_M' value (eq 6), and substrate concentrations were at least 100-fold lower. After an initial binding period, t_1, at 25 °C, 27 μL of nonradioactive product or substrate was added to initiate the chase. The duration of the initial binding period ranged from 10 to 40 s. The concentration of nonradioactive substrate during the chase ranged from 100 to 400 times the concentration of ribozyme. During the chase period, t_2, corresponding to at least 6 times the $t_{1/2}$ for the cleavage reaction, samples were removed at intervals of 10 s to 2 min and quenched. In control reactions, 2.5 μL of [5′-^{32}P]substrate was added to 5 μL of ribozyme at the same concentrations. Samples were removed from the reaction after 10 s and then at 10-s to 2-min intervals throughout the chase period. Substrate and products were quantitated as described above. Extending the chase period from 6 to 10 times the $t_{1/2}$ for the cleavage reaction produced the same cleavage extent, confirming that cleavage of bound substrate was complete during the chase period. No cleavage of radioactive substrate was detected in control experiments in which radioactive substrate was diluted into chase RNA before the addition of ribozyme, indicating that the chase conditions effectively prevented rebinding of radioactive substrate. Values for k_{-1} were calculated as described under Results.

In a typical experiment to measure the rate of substrate binding (k_1, Figure 2), separate solutions were prepared with several concentrations of ribozyme ranging from 2.5 to 320 nM, [5′-^{32}P]substrate, at a concentration of 0.5 nM, and nonradioactive substrate or product RNA at a concentration of 6400 nM. RNA solutions were denatured and preincubated in 10 mM $MgCl_2$, as described above. At t_0, 1 μL of radioactive substrate was added to 2 μL of ribozyme. At various times, t_1, 27 μL of nonradioactive chase RNA was added. Times were chosen for t_1 so that no more than 10% of the substrate had been cleaved and ranged from 6 s to 4 min. At t_2, reactions were quenched, and the amount of product was measured. The duration of t_2 corresponded to approximately 10 times the $t_{1/2}$ for the cleavage reaction, to allow complete cleavage of bound substrate, and ranged from 3.5 to 10 min. In parallel reactions, ribozyme was combined with substrate at the same concentrations and incubated for the same times, t_1, but instead of adding nonradioactive chase RNA, reactions were quenched, and the amount of product was quantitated. For each ribozyme concentration, the amount of E·S was calculated for each t_1 interval, and rate constants for substrate binding and dissociation were derived from plots of k_{obs} for E·S formation versus ribozyme concentration, as described under Results. No cleavage of radioactive substrate was detected when radioactive RNA and chase RNA were combined before the addition of ribozyme, indicating that the concentration of nonradioactive chase RNA was high enough to prevent rebinding of the radioactive substrate during the chase period.

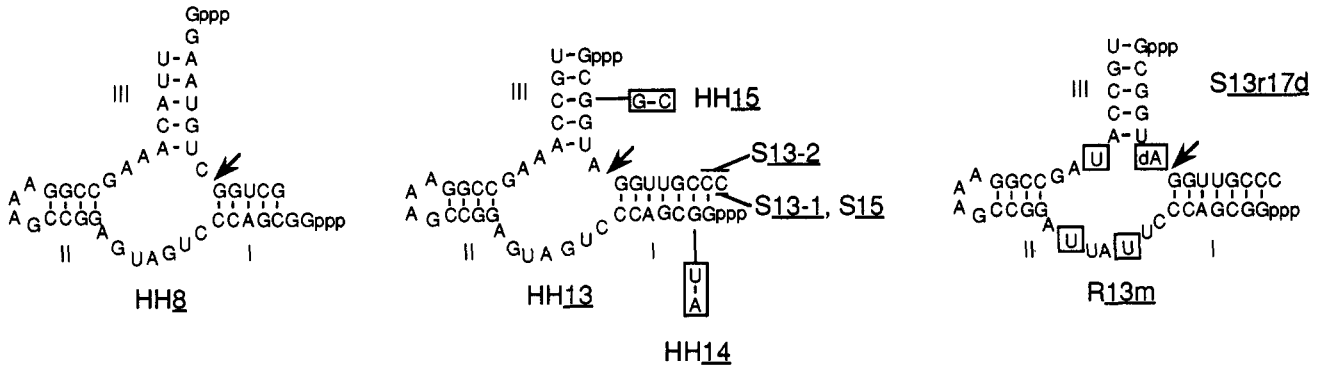

FIGURE 1: Hammerhead sequences. Each hammerhead has the same helix II sequence, five base pairs in helix III and the same unpaired nucleotides at the junction of the helices. Helix I contains five base pairs in hammerhead 8 and seven base pairs in hammerheads 13, 14, and 15. Hammerhead 14 is related to hammerhead 13 but has an A/U base pair replacing a G/C base pair in helix I. Hammerhead 15 has one G/C base pair in helix III converted to a C/G base pair, and substrate 15 lacks the 3′-terminal unpaired C residue. Substrates 13-1 and 13-2 have the same sequence as substrate 13 but lack one or two 3′-terminal cytosine residues, respectively. Ribozyme 13m contains mutations in three catalytically essential nucleotides. Substrate 13r17d contains a single deoxynucleotide residue 5′ of the cleavage site.

For hammerheads 13-1, 14, and 15, product dissociation rate constants were determined from steady-state multiple-turnover rates at saturating concentrations of substrate. To measure the dissociation rates of complexes between R13 and S13-P2 or between R13 and noncleavable substrate, S13r17d, 5 μM ribozyme was combined with 10 μM ligand. A 3-μL sample of complex was then diluted into 27 μL of 11 μM 5′-^{32}P-labeled S13. Samples were quenched and analyzed at various times ranging from 15 s to 40 min. The dissociation rate constant was derived from the slope of a plot of the amount of radioactive product formed versus time during the first turnover. At the high concentrations used, binding and cleavage of radioactive substrate were fast relative to dissociation rates so the observed rates of cleavage reflect the rates of dissociation of the noncleavable ligands. Control reactions in which ligands were combined with radioactive substrate, at the same concentrations, before the addition of ribozyme displayed kinetics that were indistinguishable from those of reactions with ribozyme and radioactive substrate alone, indicating that the concentration of radioactive substrate added during the chase was sufficiently high to prevent rebinding of the ligand.

The dissociation rate of a complex between inactive ribozyme, R13m, and substrate was measured in similar experiments except that the initial complex was formed by combining 2 μL of 9 μM R13m with 1 μL of [5′-^{32}P]substrate. After an initial binding period of 20 s, 3 μL of complex was diluted into 27 μL of 6.6 μM active R13. The rate of dissociation of the inactive complex was derived from a plot of ln (fraction S) versus time during the chase. When radioactive substrate was added to a solution containing inactive ribozyme and active ribozyme at the same concentrations present during the chase period, observed cleavage rates were the same as in parallel reactions that contained active ribozyme alone. Therefore, the concentration of active ribozyme was sufficiently high to prevent rebinding of the inactive ribozyme during the chase.

Kinetic parameters measured in similar experiments typically varied less than 2-fold.

Measurement of Equilibrium Dissociation Constants for Inactive Hammerhead Complexes. Equilibrium dissociation constants were measured using nondenaturing gel electrophoresis similar to the method developed by Pyle et al. (1990). Separate solutions of ribozyme and 5′-^{32}P-end-labeled inactive substrate or product were heated for 1 min at 95 °C in 50 mM Tris-HCl, pH 7.5/5% sucrose/0.02% bromophenol blue/0.02% xylene cyanol and then adjusted to a final concentration of 10 mM $MgCl_2$ and allowed to incubate at 25 °C for 15 min. Ribozyme and ligand were then combined and allowed to incubate at 25 °C for 15 h to 3 days. Experiments with longer and shorter incubation times were compared to verify that equilibrium had been attained.

Each experiment included 12–16 ribozyme concentrations ranging from approximately 0.2 nM to a concentration that was at least 10-fold higher than the K_d value and radioactive ligand concentrations that were at least 10-fold below the lowest ribozyme concentration. To correct for the fraction of ligand present in secondary structures that were unable to bind ribozyme even at saturating concentrations, the fraction of radioactive ligand bound at each ribozyme concentration was normalized to the extent of binding observed at a ribozyme concentration that was 100-fold higher than the K_d value. For long incubation times, reaction mixtures were centrifuged at intervals to prevent changes in concentration due to evaporation. Omission of bromophenol blue and xylene cyanol had no detectable effect on equilibrium dissociation constants.

Bound and unbound ligand were separated using nondenaturing polyacrylamide gel electrophoresis carried out under buffer and temperature conditions similar to those used for kinetic experiments. Acrylamide gels (15%, with a 19:1 ratio of acrylamide to bisacrylamide, 40 × 25 × 0.15 cm) in 50 mM Tris acetate, pH 7.5/10 mM magnesium acetate buffer were subjected to pre-electrophoresis for 2 h at 20 W. The electrophoresis buffer was replaced, and samples were subjected to electrophoresis at 15 W for 4 h at room temperature. Quantitation of free and bound ligand was carried out using a Molecular Dynamics radioanalytic scanner or by scintillation counting of excised bands. To ensure that product or substrate that dissociated from a complex during electrophoresis was measured as complex rather than free ligand, the fraction of free ligand at each concentration was determined from the ratio of radioactivity in the band corresponding to free ligand to the total radioactivity in the lane. K_d values were determined by computing the fit to theoretical binding curves.

RESULTS

The hammerheads examined in these experiments (Figure 1) consist of a large ribozyme RNA, with most of the conserved nucleotides, and a small substrate RNA that contains the cleavage site. These hammerheads have the same essential unpaired nucleotides at the junction of the helices and the same helix II sequence but differ in the length and sequence of helices I and III formed between the ribozyme and the

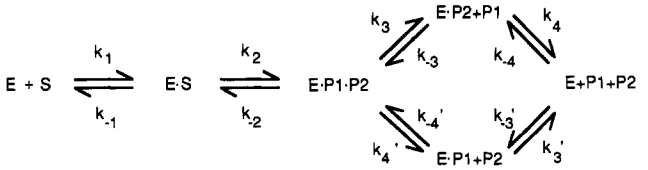

FIGURE 2: Minimal kinetic mechanism for intermolecular hammerhead catalysis.

substrate. Substrate 8 (S8) binds ribozyme 8 (R8) through two five base-pair helices whereas S13 is bound through helix I with seven base pairs and helix III with five base pairs. S13-1 and S13-2 have the same sequence as S13 but lack one or two 3′-terminal C residues, respectively. Hammerhead 14 (HH14) has the same sequence as HH13 except that an A/U base pair is substituted for a G/C base pair in helix I of HH14. A G/C base pair is inverted in helix III of HH15, and S15 also lacks one 3′-terminal C residue. Steady-state kinetic parameters have been reported for HH8 (Fedor & Uhlenbeck, 1990), and the structure of R8 has been examined using NMR (Heus et al., 1990). NMR experiments have identified three base-paired helices in a complex of R13 and a complementary DNA substrate analog (Heus & Pardi, 1990).

R13m is a variant of R13 in which three purines that are essential for catalytic activity (Ruffner et al., 1990) were mutated to U residues. Using standardized hammerhead nomenclature (Hertel et al., 1992) R13m is R13 G4U, G8U, A14U. As expected, saturating concentrations of R13m displayed no detectable catalytic activity even after incubation with S13 for 8 h. S13r17d is a variant of S13 which has a single deoxynucleotide at the cleavage site. As previously reported for similar substrates (Perreault et al., 1990; Dahm & Uhlenbeck, 1990), S13r17d is inactive in cleavage.

A minimal mechanism for hammerhead cleavage (Figure 2) includes substrate binding (k_1), cleavage (k_2), and release of both products (k_3 and k_4) as well as the reverse reactions of substrate dissociation (k_{-1}), product ligation (k_{-2}), and product binding (k_{-3} and k_{-4}). We measured rate constants for steps in the forward direction as well as k_{-1}. Equilibrium dissociation constants (K_d) were also measured for catalytically inactive hammerhead complexes.

The Rate Constant for Hammerhead Cleavage. Two types of experiments, with either substrate or ribozyme in excess, were used to measure the cleavage rate constants for hammerheads 8 and 13. In the first, various concentrations of radioactive substrate were combined with one-tenth the concentration of ribozyme. The amount of product was measured as a function of time through the first 5% of the reaction to obtain the initial velocity. These cleavage rate constants therefore reflect only the first turnover and not subsequent turnovers that require release of products to regenerate free ribozyme. The second type of experiment determined the cleavage rate constant from pseudo-first-order reactions using a trace amount of radioactive substrate and various concentrations of ribozyme in excess of substrate. For each type of experiment, eight cleavage rates were measured spanning at least an 80-fold range of concentrations of substrate or ribozyme.

The single-turnover rates of cleavage were plotted as a function of substrate concentration or ribozyme concentration in Eadie–Hofstee type plots (Eadie, 1942; Hofstee, 1952) to obtain k_2 values from the Y-intercept and K_M' values from the slope (Table I). Because these measurements pertain to single-turnover rather than multiple-turnover reactions and because some of these reactions do not follow a Michaelis–Menten kinetic scheme (see below), the concentration at which the reaction velocity was half maximal is termed K_M' since it is not a true Michaelis constant. Substrate-excess and ribozyme-excess experiments gave virtually the same values for k_2 and K_M'. For example, hammerhead 8 gave k_2 = 1.0 min^{-1} and K_M' = 41 nM in substrate-excess experiments and k_2 = 1.4 min^{-1} and K_M' = 49 nM in ribozyme-excess experiments. Due to potential difficulties in distinguishing the first and second turnover phases inherent in substrate-excess experiments, the k_2 and K_M' values from ribozyme-excess experiments are likely to be more reliable and are therefore reported in Table I. The hammerhead sequences described here displayed k_2 values from 1.2 to 2.0 min^{-1} which are similar to k_{cat} values reported previously for other hammerhead sequences (Uhlenbeck, 1987; Fedor & Uhlenbeck, 1990; Table I). Since these rate constants were derived from the first turnover, they reflect the rate-determining step that precedes product release which, in a minimal kinetic mechanism, is cleavage chemistry.

Table I: Kinetic Parameters for Hammerhead Cleavage

hammerhead	k_{cat} (min^{-1})[a]	K_M' (nM)[b]	k_2 (min^{-1})[b]	k_2/K_M' (μM^{-1} min^{-1})
8	1.4	49	1.4	29
13	0.028	96	1.2	12
14	0.11	52	1.9	36
15	0.036	100	2.0	20
13-1	0.053	88	1.2	14
13-2	1.4	57	1.4	25

[a] Multiple-turnover cleavage rates at saturating concentrations of substrate. [b] Values obtained from plots of cleavage rates (k_{obs}), versus k_{obs}/[R] in experiments with various concentrations of ribozyme [R] and trace amounts of [5′-^{32}P]substrate.

The Rate Constant for Substrate Dissociation. Substrate dissociation rate constants were measured in partitioning experiments (Rose et al., 1974). First, ribozyme and a trace amount of radioactive substrate were combined at a sufficiently high ribozyme concentration for a period, t_1, that was long enough to ensure complete binding. The ribozyme–substrate complex was then diluted into a large excess of nonradioactive substrate or product RNA, and cleavage of radioactive substrate was measured during the chase period. Radioactive substrates that are weakly bound will dissociate from the ribozyme during the chase and be replaced by nonradioactive substrate so that no more radioactive product will form. Strongly bound substrates will remain bound to the ribozyme and will go on to cleave during the chase period. For hammerhead 8, almost no further radioactive product formed during the chase period indicating that substrate dissociation was fast relative to cleavage and could not be measured using this assay (Figure 3A). The small amount (less than 10%) of substrate that appeared to cleave after the addition of nonradioactive chase RNA probably reflects cleavage during the few seconds required for complete mixing. In contrast, hammerheads 13 (Figure 3B), 14 (Figure 3C), and 15 (Figure 3D) showed substantial conversion of radioactive substrate to product during the chase, indicating that substrate dissociation was slow relative to cleavage. S13-1, which has the same sequence as S13 but lacks a 3′ unpaired cytosine residue, dissociated slightly faster than S13 (Figure 3E), and S13-2, which lacks two 3′-terminal cytosine residues and thus forms one less base pair with the ribozyme, dissociated completely during the chase (Figure 3F).

The rate constants for substrate dissociation were calculated by comparing chase and control reactions in two ways. The first makes use of the fact that the extent of the reaction was lower in the chase experiment than in the reaction without the

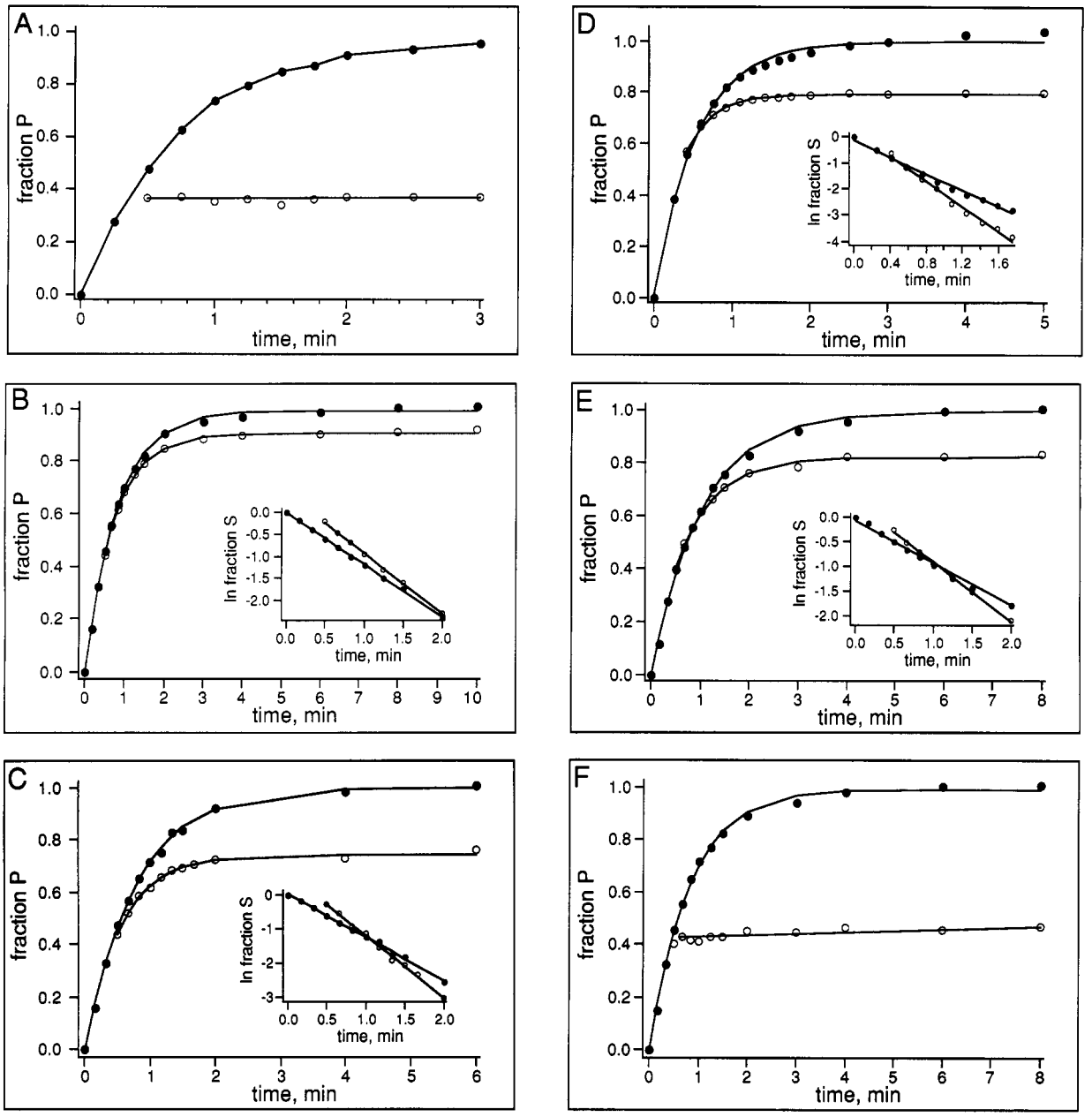

FIGURE 3: Chase experiments to determine substrate dissociation rate constants, k_{-1}. (A) The fraction of substrate converted to product at various times is shown for a reaction in which 1.0 μM R8 was combined with a trace amount of [5′-^{32}P]S8. After 15 s, t_1, the reaction was diluted into 40 μM nonradioactive chase S8 (○), or the reaction was allowed to proceed without the chase (●). The fraction of S8 that was present at t_1 but failed to cut during the chase reaction was less than 0.1. (B) 6 μM R13 was combined with a trace amount of [5′-^{32}P]S13. At t_1 = 20 s, the reaction was diluted into 60 μM nonradioactive S13-P2 (○), or the reaction was allowed to proceed without the chase (●). The fraction of S13 that was present at t_1 and failed to cut during the chase reaction was 0.86. Plots of ln (fraction S) versus time give k_{obs} values of 1.17 and 1.40 min^{-1} for control (●) and chase (○) reactions, respectively (inset). (C) An experiment similar to that shown in panel B except that R14 and [5′-^{32}P]S14 were combined during t_1 and diluted into 90 μM nonradioactive S14 for the chase period. The fraction of S14 that was present at t_1 and failed to cut during the chase reaction was 0.61. Plots of ln (fraction S) versus time give k_{obs} values of 1.28 and 1.82 min^{-1} for control (●) and chase (○) reactions, respectively (inset). (D) R15 and [5′-^{32}P]S15 were combined during t_1 and diluted into 60 μM S13-P2 to initiate the chase. The fraction of S15 that was present at t_1 and failed to cut during the chase reaction was 0.67. Plots of ln (fraction S) versus time give k_{obs} values of 1.60 and 2.43 min^{-1} for control (●) and chase (○) reactions, respectively (inset). (E) R13 and [5′-^{32}P]S13-1 were combined during t_1 and diluted into 60 μM S13-P2 to initiate the chase. The fraction of S13-1 that was present at t_1 and failed to cut during the chase reaction was 0.76. Plots of ln (fraction S) versus time give k_{obs} values of 0.85 and 1.21 min^{-1} for control (●) and chase (○) reactions, respectively (inset). (F) R13 and [5′-^{32}P]S13-2 were combined during t_1 and diluted into 60 μM S13-P2 to initiate the chase. The fraction of S13-2 that was present at t_1 and failed to cut during the chase reaction was less than 0.2.

chase because a fraction of the substrate dissociated rather than cleaved. The fraction of substrate that goes on to cleave after the initial binding period is proportional to the cleavage and substrate dissociation rate constants.

$$[P^*]_\infty/([P^*]_\infty + [S^*]_\infty) = k_2/(k_2 + k_{-1}) \quad (1)$$

$[P^*]_\infty$ and $[S^*]_\infty$ are the amounts of radioactive product and substrate, respectively, present at the end of the chase period after subtracting the amount of substrate that was converted to product during the initial binding phase. The second calculation is based on comparison of cleavage rates in the presence and absence of the chase. The chased reaction is completed more quickly than the control reaction since less substrate is cleaved by the endpoint. Since E·S decays through dissociation as well as cleavage, the observed reaction rate is faster by the value of k_{-1}:

Table II: Substrate Binding and Dissociation Rate and Equilibrium Constants

ribozyme	substrate	k_{-1} (min^{-1})	k_1 (μM^{-1} min^{-1})	K_d (nM)
R8	S8	fast		49[b]
R13	S13	0.23 ± 0.07	9.1	23[c]
R14	S14	0.67 ● 0.16	84	14[c]
R15	S15	0.81 ± 0.20	29	29[c]
R13	S13-1	0.31 ± 0.05		18[c]
R13	S13-2	fast		57[c]
R13	S13r17d	0.011 ± 0.005	16[a]	0.7 ± 0.4
R13m	S13	0.0005 ■ 0.0002	2.5[a]	0.2 ± 0.1
R13m	S13r17d			2.0 ± 1.0

[a] Calculation based on k_{-1} and K_d measurements. [b] K_M. [c] Calculation based on K_M', k_2, and k_{-1} measurements.

$$k_{obs} = k_2 + k_{-1} \quad (2)$$

The slopes of plots of ln (fraction S) versus time give k_2 for cleavage in the absence of a chase and k_{obs} for cleavage during the chase. For hammerhead 13, calculations using eqs 1 and 2 produced k_{-1} values of 0.23 min^{-1}. Analogous experiments with hammerheads 14 and 15 showed slightly faster dissociation rate constants, and values obtained using each equation agreed within 25% (Table II). By assuming that the small amount of S8 that appeared to cleave during the chase reflected cleavage of bound substrate and was not an artifact of "slow" mixing, a lower limit of 12 min^{-1} can be set for the S8 dissociation rate constant using eq 1.

Since the values of k_{-1} for hammerheads 13–15 were considerably faster than expected (see Discussion), several experiments were carried out to examine the validity of the chase protocol for determining the rate of substrate dissociation. A major concern was that some of the substrate did not bind ribozyme during t_1 and therefore failed to cleave during the subsequent chase. If this happened, the value of k_{-1} would be overestimated. Although binding should have been complete with 6 μM R13 and a t_1 of 20 s, the experiment in Figure 3B was repeated with a range of ribozyme concentrations and initial binding times. Decreasing the concentration of R13 to 2 μM or increasing it to 16 μM did not change the value of k_{-1} when t_1 was 20 s. If binding was incomplete during t_1 due to an unexpectedly slow rate of binding, the amount bound and the fraction cleaved during the chase would have increased with increasing R13 concentration. Thus, R13 is saturated for binding in 20 s. While t_1 could not be varied as much and still obtain accurate data, experiments varying t_1 from 10 to 40 s did not change the value of k_{-1}. This also suggests that the ribozyme–substrate complex was fully formed during t_1.

Another potential artifact of measuring substrate dissociation through partitioning experiments is that the nonradioactive chase RNA could affect k_{obs} and the extent of the reaction by combining with the ribozyme–substrate complex to form a ternary complex. Ternary complex formation could either reduce the cleavage rate or accelerate the dissociation of radioactive substrate through a branch migration mechanism. If this were the case, the chase experiment in Figure 3B might be affected by the concentration of nonradioactive chase RNA. However, k_{-1} was the same when the concentration of nonradioactive chase RNA was 20 or 160 μM. The propensity to form a ternary complex might be expected to depend on the sequence or size of the chase RNA. However, when nonradioactive S13-1, S13-2, S15, or S13-P2, the 3′ product of S13 cleavage, was used as the chase RNA, the results were the same.

An attempt was made to verify k_{-1} values by monitoring the decay of ribozyme–substrate complexes using nondenaturing gel electrophoresis. Pulse–chase experiments were carried out as described above except that samples were applied to nondenaturing gels at intervals throughout the chase period. Although the expected amount of radioactive product was seen, no evidence of a ribozyme–substrate complex was found so k_{-1} values could not be measured this way. The failure to detect ribozyme–substrate complexes by nondenaturing gel electrophoresis was nonetheless consistent with the rapid k_{-1} values determined kinetically; a ribozyme–substrate complex that decayed on the order of 0.2 min^{-1} would not be stable enough to persist through lengthy gel electrophoresis. Furthermore, since no slowly migrating species containing radioactive substrate was detected, nondenaturing gel electrophoresis experiments appear to rule out ternary complex formation.

The Rate Constant for Substrate Binding. Since reaction rates at low concentrations can be no faster than complex formation, values for k_2/K_M' (Table I) define lower limits for substrate binding rate constants. Values for k_2/K_M' ranged from 12 μM^{-1} min^{-1} for hammerhead 13 to 36 μM^{-1} min^{-1} for hammerhead 14 (Table I).

The second-order rate constant for substrate binding was also measured directly using pulse–chase experiments. When ribozyme and substrate are first combined, the fraction of substrate present in E·S will increase until equilibrium is achieved. At early times in the reaction, before a significant amount of substrate has been converted to product, the concentrations of ribozyme, substrate, and hammerhead complex will approach an equilibrium where the rate of substrate binding is equal to the rate of dissociation. The rate of approach to equilibrium will equal the sum of the forward and reverse rates:

$$k_{obs} = k_1[E] + k_{-1} \quad (3)$$

To measure the rate of approach to equilibrium, it is necessary to measure the amount of E·S formed as a function of ribozyme concentration and time. Because the ribozyme–substrate complex cannot be measured directly, a chase period was used to allow conversion of E·S to E·P1·P2, which can be measured (Figure 4A). The amount of product formed by the end of the chase will not reflect the amount of E·S at t_1 directly because a portion of substrate will dissociate rather than cleave. As described in the analysis of substrate dissociation rates (above), the amount of product formed during the chase will be proportional to the amount of ribozyme–substrate complex present at the start of the chase by the ratio $k_2/(k_2 + k_{-1})$. For example, if cleavage and substrate dissociation rates were equal, half of the substrate bound to ribozyme at t_1 would be converted to product and half would dissociate during t_2. The amount of E·S present at t_1 could therefore be determined by doubling the amount of product formed during t_2. The amount of product formed during the chase multiplied by $(k_2 + k_{-1})/k_2$ plus the amount of product formed before the chase began were used to calculate values for the amount of E·S formed by t_1:

$$F(E\cdot S)_{t_1} = F(P)_{t_1} + [F(P)_{t_2} - F(P)_{t_1}]\left[\frac{(k_2 + k_{-1})}{k_2}\right] \quad (4)$$

An example of an experiment to measure the observed rate of E·S formation with 120 nM R13 is shown in Figure 4B. The reaction was initiated by combining 120 nM R13 with a trace amount of [5′-^{32}P] S13. Then, at various times, t_1, after the start of the reaction, the amount of product was

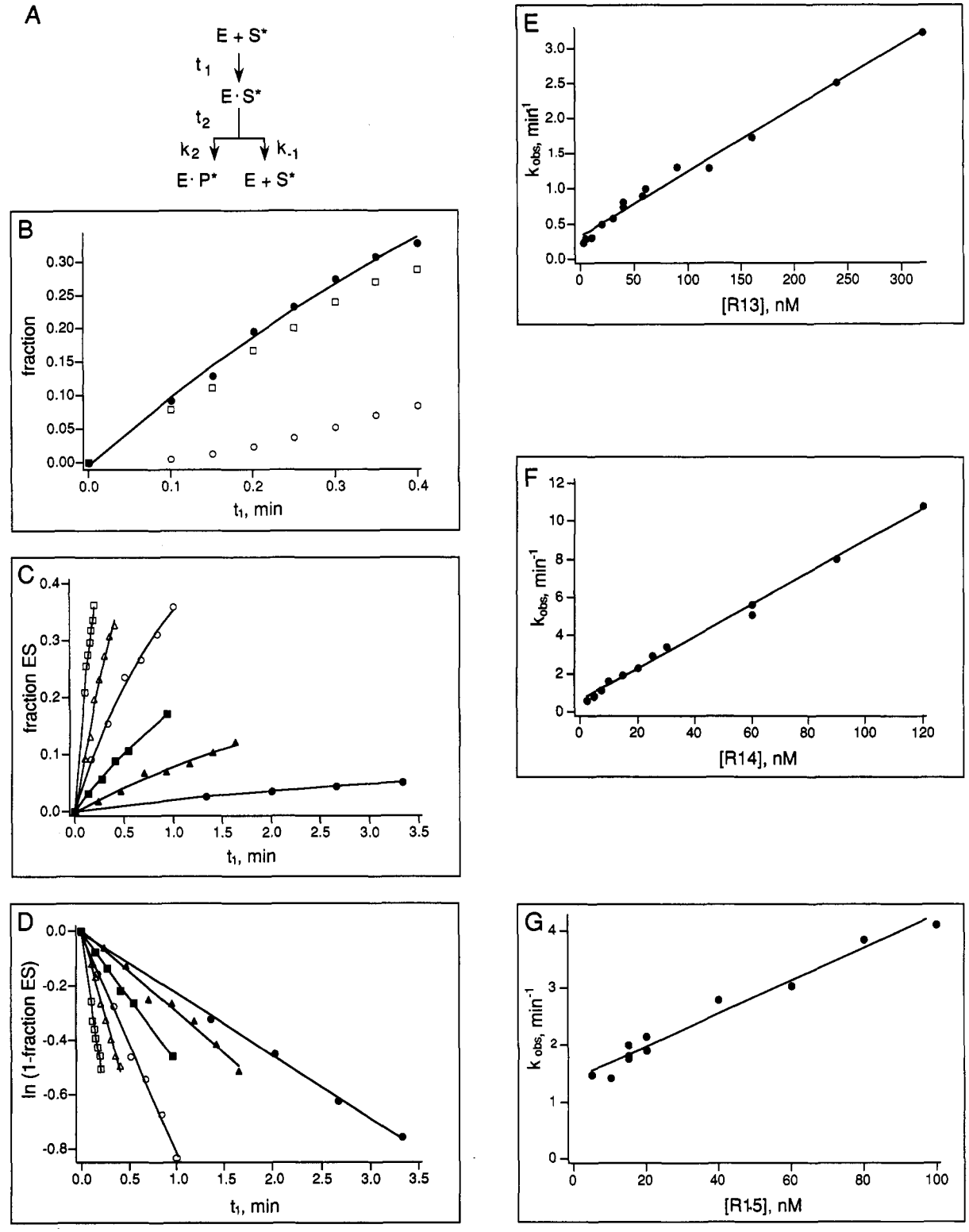

FIGURE 4: Determination of rate constants for substrate binding. (A) Pulse-chase protocol. (B) Fraction of product formed plotted as a function of time during t_1 (○) and t_2 (□) and fraction of E·S formed during t_1 (●), calculated as described in the text, with hammerhead 13 at a concentration of 120 nM. (C) Plot of the fraction of S13 present in E·S as a function of time, t_1, and lines representing the best fit of fraction E·S values to an exponential curve, for R13 at concentrations of 2.5 (●), 10 (▲), 20 (■), 40 (○), 120 (△), and 240 nM (□). (D) Logarithmic plot of data shown in panel C, used to calculate k_{obs} for ES formation. (E) Plot of R13 concentration versus k_{obs} for hammerhead 13 complex formation. The slope of 9.1 μM^{-1} min^{-1} gives the rate constant for S13 binding, and the Y-intercept of 0.32 min^{-1} corresponds to the rate constant for S13 dissociation. (F) Plot of R14 concentration versus k_{obs} for hammerhead 14 complex formation. The slope of 84 μM^{-1} min^{-1} gives the rate constant for S14 binding, and the Y-intercept of 0.57 min^{-1} corresponds to the rate constant for S14 dissociation. (G) Plot of R15 concentration versus k_{obs} for hammerhead 15 complex formation. The slope of 29 μM^{-1} min^{-1} gives the rate constant for S15 binding, and the Y-intercept of 1.4 min^{-1} corresponds to the rate constant for S15 dissociation.

measured (open circles). These values represent E·S that was converted to E·P1·P2 during t_1. In a parallel reaction, an excess of nonradioactive product was added at t_1 and followed by a chase period, t_2, before product was measured (open squares). These values represent the amount of product that had formed by t_1 plus the amount of E·S present at t_1 that was converted to E·P1·P2 during the chase period. The amount of product formed between t_1 and t_2 was multiplied by the

factor 1.19, corresponding to $(k_2 + k_{-1})/k_2$ for hammerhead 13, to correct for the amount of substrate that was bound to ribozyme at t_1 but dissociated rather than cleaved during t_2. This value for the amount of E·S at t_2 was added to the fraction of product formed by t_1 to obtain a value for the total fraction of substrate that had formed E·S by t_1 (solid circles). This experiment was carried at several R13 concentrations (Figure 4C). Semilogarithmic plots of 1 – fraction(E·S) versus time were used to determine k_{obs} for E·S formation at each concentration of ribozyme (Figure 4D). Endpoints used in these rate calculations were derived from eq 5, where FB_∞ is

$$FB_\infty = [E]/([E] + K_d) \quad (5)$$

the fraction of substrate bound to ribozyme at equilibrium. K_d values (Table II) were calculated from measured values for K_M', k_2, and k_{-1}, using

$$K_M' = (k_{-1} + k_2)/k_1 \quad (6)$$

A plot of k_{obs} for E·S formation versus ribozyme concentration will have a slope equal to the second-order rate constant for substrate binding and a Y-intercept equal to the substrate dissociation rate constant (eq 3). A second-order rate constant for S13 binding of 9.1 μM^{-1} min^{-1} and a dissociation rate constant of 0.32 min^{-1} were obtained (Figure 4E). Similar experiments with hammerheads 14 and 15 are shown in Figure 4F,G (Table II).

Values for k_{obs} might be overestimated using these calculations if k_{-1} values had been overestimated and yielded K_d values that were too high. To evaluate the possible effect of such an error, a second calculation was carried out assuming that the fraction of substrate present as complex at equilibrium was 1, as would be the case if K_d values were actually quite low. Values for k_1 that were determined from the slope of plots analogous to those in Figure 4E–G, but using an endpoint of 1 for calculating k_{obs} values, agreed within 15% with values obtained with endpoints derived from calculated K_d values. However, the Y-intercepts of such plots were near zero instead of near the k_{-1} values that had been measured previously. Consequently, these experiments yielded k_1 values more or less independent of assumptions regarding K_d values for hammerhead complexes but provide a poor measure of k_{-1}.

The Rate Constants for Product Dissociation, k_3 and k_4. After a substrate molecule is cleaved, the two products must be released from the ribozyme to allow the next molecule of substrate to bind. For hammerhead 8 and three hammerheads that also have five base pairs in helices I and III, little (less than 2-fold) difference was seen between the rates of the first and subsequent turnovers (Fedor & Uhlenbeck, 1990). Similarly, the hammerhead formed between R13 and S13-2 displayed virtually no difference between single- and multiple-turnover rates. These observations indicate that, for these hammerheads, product release occurred at a rate faster than or on the same order as cleavage chemistry. In contrast, substrates 13, 13-1, 14, and 15 form helices of five and seven base pairs with their corresponding ribozymes and display quite different kinetic behavior. At saturating substrate concentrations and an excess of substrate over ribozyme, all four display a "burst" of product formation at a rate quite close to k_2 followed by a much slower steady-state rate. At a constant, saturating concentration of substrate, the amount of product formed during the "burst" was directly proportional to the ribozyme concentration (shown for HH13 in Figure 5A). This is consistent with the onset of the slow phase of the reaction corresponding to the transition from single to multiple turnovers. S15 and S13-1, which have the same seven base

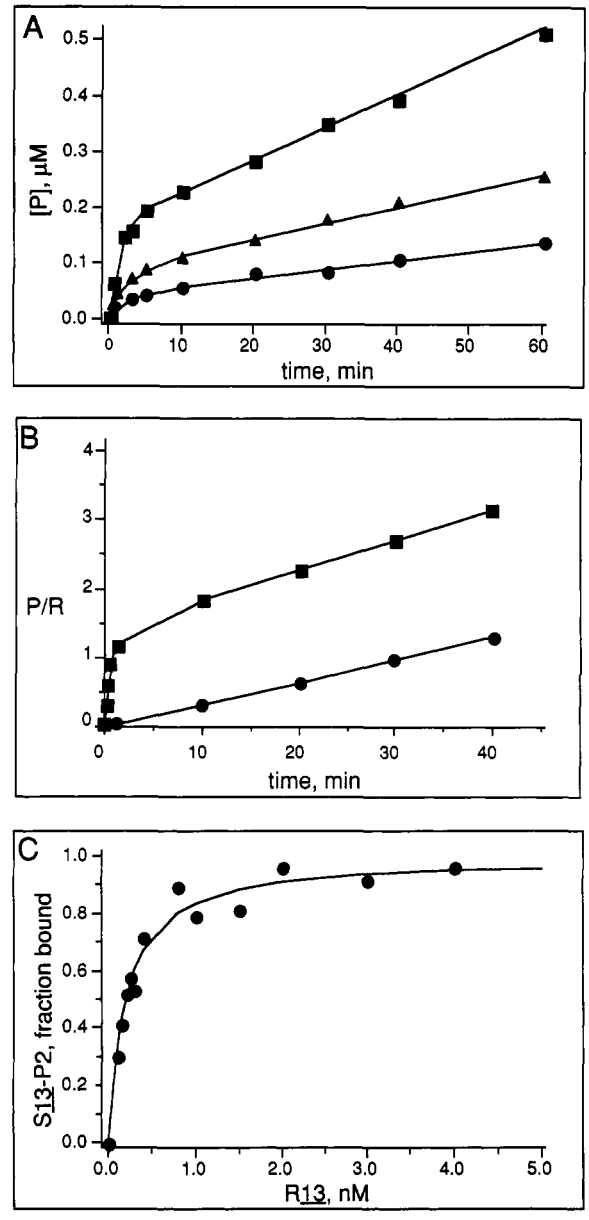

FIGURE 5: Analysis of product release for hammerhead 13. (A) The concentration of product as a function of time for reactions initiated with 6 μM S13 and R13 at a concentration of 0.05 (●), 0.1 (▲), or 0.2 μM (■). (B) Determination of the rate constant for product dissociation, k_4. The concentration of product, normalized to ribozyme concentration, is shown for reactions containing 0.2 μM R13 and 2.0 μM S13 with (●) or without (■) preincubation of ribozyme with 0.3 μM of the 3′ product of S13 cleavage (S13-P2). The cleavage rate measured after preincubation with S13-P2 was 0.025 min^{-1}, and the multiple-turnover rate for the reaction with no preincubation was 0.028 min^{-1}. (C) Equilibrium dissociation constant for a complex containing R13 and S13-P2, determined by measuring the fraction of [5′-^{32}P]S13-P2 bound in the presence of various concentrations of R13 by nondenaturing gel electrophoresis. The line represents the calculated best fit of the data to an ideal binding curve corresponding to a K_d value of 0.2 nM.

P2 sequence as S13 but a lack an unpaired C residue at their 3′ termini, showed slightly faster multiple-turnover rates than S13 (Table III). Hammerhead 14, in which a G/C base pair in the P2 helix of hammerhead 13 was replaced by a weaker A/U base pair, displayed a multiple-turnover rate that was about 4-fold faster than for S13 but still nearly 20-fold slower than its k_2 value. These data suggest that the slow multiple-turnover rates of hammerheads 13 – 15 are determined by the rate of product release and the longer P2 product appears to contribute substantially.

Table III: Dissociation Rate Constants and Equilibrium Dissociation Constants for Ribozyme–Product Complexes

ribozyme	ligand	k_4 (min^{-1})[a]	K_d (nM)[b]	fraction active ribozyme[c]
R13	S13-P2	0.028 ± 0.002	0.5 ± 0.3	0.94 ± 0.06
R13	S13-1-P2	0.053 ± 0.013		0.91 ± 0.2
R13m	S13-P2		0.4 ± 0.2	
R14	S14-P2	0.11 ± 0.02		0.97 ± 0.06
R15	S15-P2	0.036 ± 0.006		0.85 ± 0.07

[a] Average multiple-turnover cleavage rates with 6 μM substrate and three ribozyme concentrations ranging from 0.05 to 0.2 μM. [b] Average of four determinations. [c] Calculation based on the amount of product formed per mole of ribozyme during the first turnover from reactions described in footnote a.

To distinguish whether the multiple-turnover rate was due solely to dissociation of P2 or whether dissociation of both products contributed, the rates of decay of complexes between each S13 product and the ribozyme were measured directly. When R13 was preincubated with purified S13-P2 before adding radioactive substrate, no "burst" occurred and radioactive products appeared at the multiple-turnover rate from the onset of the reaction (Figure 5B). In contrast, preincubation of R13 with S13-P1, at concentrations as high as 1 μM, had no effect on initial or multiple-turnover rates after radioactive substrate was added. This indicates that the multiple-turnover rate for hammerhead 13 is determined by k_4, the rate of release of S13-P2. The value of k_3, the rate of release of S13-P1, appears to be considerably faster and therefore does not contribute to the multiple-turnover rate. This conclusion was confirmed by combining R13 and radioactive S13 and analyzing the products on a nondenaturing gel. A low mobility species was observed that depended on the presence of R13 and contained S13-P2 but not S13-P1, further evidence that a stable complex formed between R13 and S13-P2.

Equilibrium dissociation constants for the complex of R13 and S13-P2 were measured directly by combining various concentrations of ribozyme with trace amounts of radioactive S13-P2 and fractionating bound from free S13-P2 using nondenaturing gel electrophoresis (Pyle et al., 1990). A K_d value of 0.5 nM for the R13 – S13-P2 complex was determined by the fit to a theoretical binding curve (Figure 5C). No complex was detected between R13 and S13-P1 even at ribozyme concentrations as high as 20 μM. Taken together, these experiments indicate that release of S13-P1 occurs rapidly upon cleavage (k_3) and is followed by slow release of S13-P2 (k_4) which is rate-determining for multiple-turnover reactions at saturating substrate concentrations.

The large difference between single- and multiple-turnover rates for hammerheads 13, 14, and 15 permits a titration to determine the fraction of active ribozyme. The amount of product formed during the first turnover in the experiment shown in Figure 5B was determined by extrapolating the multiple-turnover rate to $t = 0$. The active fraction of R13 was approximately 0.9 since 0.9 equiv of product per equivalent of ribozyme was formed in the first turnover. Similar active site titrations with hammerheads 14 and 15 revealed the fraction of active ribozyme to be approximately 1.0 and 0.9, respectively (Table III). These active site titrations rule out the possibility that catalytic activity is due to a rare species in these ribozyme preparations since most of each ribozyme was active. Active fractions less than 1 might reflect the presence of inactive ribozyme conformations or inaccuracy of RNA concentration estimates.

The Stability of Inactive Ribozyme–Substrate Complexes. Comparison of S13-P2 and S13 dissociation rates reveals the surprising result that product dissociates from the ribozyme more slowly than the corresponding substrate that forms five additional base pairs with the ribozyme. Association rates would be expected to increase and dissociation rates would be expected to decrease with length for a simple RNA duplex, so that larger duplexes should be more stable (Porschke & Eigen, 1971; Craig et al., 1971; Porschke et al., 1973; Ravetch et al., 1974; Breslauer & Bina-Stein, 1977; Nelson & Tinoco, 1982). However, for S13, S13-1, S14, and S15, substrate dissociation rates were found to be 6–20-fold faster than corresponding dissociation rates of P2. This suggests that the ribozyme–substrate complex is less stable than the ribozyme–product complex.

If the difference in the stability of E·S and E·P2 is related to the catalytic properties of the hammerhead, this difference might disappear with catalytically inactive hammerhead complexes. To test this possibility, dissociation rate constants were measured for two types of complexes that were catalytically inactive due to alterations of either the substrate or the ribozyme. The first experiment was carried out by combining R13 with S13r17d, at concentrations sufficiently high to promote rapid and complete binding, and then diluting the complex into an excess of [5′-^{32}P]S13. Since S13 binding and cleavage are relatively fast at high concentrations, the observed rate of S13 cleavage reflects the rate at which ribozyme dissociated from S13r17d and became free to bind and cleave S13. The S13r17d dissociation rate constant measured in this fashion was 0.01 min^{-1}, a rate that was 20-fold slower than the rate of S13 dissociation measured previously (Table II).

The rate constant for S13 dissociation from inactive R13m was measured in a complementary experiment. A high concentration of R13m was combined with a small amount of [5′-^{32}P]S13 for 20 s. The complex was then diluted into a large excess of R13. The observed cleavage rate will reflect the rate at which the substrate dissociated from R13m and became free to bind R13. The measured rate constant of 0.0005 min^{-1} was 460-fold slower than the rate of substrate dissociation from active ribozyme (Table II). This experiment also serves as an important control for partitioning experiments used to measure the rate of substrate dissociation from active ribozyme (Figure 3B). If a portion of the S13 had not bound to R13m in the initial 20-s incubation, it would have been rapidly cleaved after R13 was added. However, less than 4% of S13 was cleaved 10 min after dilution into R13. This suggests that virtually all of the S13 would bind to R13 in the 20-s t_1 interval used in the partitioning experiment shown in Figure 3B.

Control experiments were carried out to ensure that the rates of cleavage during the chase did not result from competitive inhibition by the relatively low concentration of R13m or S13r17d that remained during the chase. Although the inactive RNAs were diluted 10-fold during the chase, competitive inhibition could still occur if the inactive RNAs bound significantly faster than their functional counterparts. However, when the inactive RNAs were combined with functional RNAs before the addition of cleavable substrate or catalytically active ribozyme, observed cleavage rates were the same as for parallel reactions containing no nonfunctional RNAs. These control experiments confirmed that the observed rates corresponded to slow dissociation of inactive complexes rather than inhibition by the inactive RNAs.

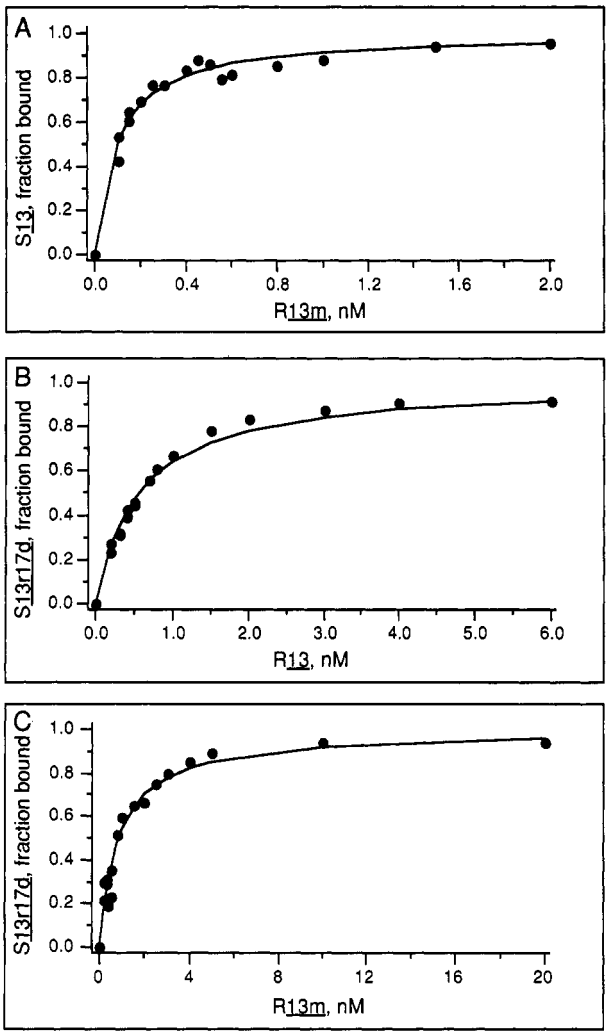

FIGURE 6: Determination of equilibrium dissociation constants for catalytically inactive ribozyme–substrate complexes. The fraction of substrate bound is shown as a function of ribozyme concentration for R13m and S13 (A), R13 and S13r17d (B), and R13m and S13r17d (C). The lines represent calculated best fits of the data to ideal binding curves corresponding to K_d values of 0.1 (A), 0.6 (B), and 1.0 nM (C).

To confirm the enhanced stability of inactive hammerhead complexes relative to active complexes that was inferred from comparison of dissociation rate constants, equilibrium dissociation constants for inactive complexes were determined directly. The equilibrium dissociation constant for the complex containing R13 and S13r17d was found to be 0.7 nM, and the complex between the inactive R13m and S13 had a K_d value of 0.2 nM (Figure 6, Table II). These K_d values agree well with dissociation rate constants determined kinetically if binding rate constants are assumed to be 16 μM^{-1} min^{-1} and 2.5 μM^{-1} min^{-1} for S13r17d and R13m, respectively, rate constants on the same order as those measured for functional complexes (Table II). Thus, K_d values for both inactive E·S complexes were substantially lower than the K_d value of 23 nM calculated from substrate binding and dissociation rate constants for the active complex. In contrast, complexes containing S13-P2 and active or inactive ribozymes were nearly equally stable, with K_d values of 0.5 and 0.4 nM, respectively (Figure 5C, Table III). Therefore, inactivating mutations in the ribozyme stabilized E·S without affecting E·P. Since complexes that contained the substrate analog or the mutationally inactivated ribozyme were more stable than the active complex, the lower stability of E·S compared to E·P was characteristic only of functional hammerhead complexes.

DISCUSSION

Kinetic characterization of six related hammerheads revealed large differences in binding and dissociation rates with correspondingly large effects on the steady-state kinetics of cleavage; however, differences in substrate length and sequence had little effect on the rate of the cleavage step. The similarity in k_2 values among a variety of hammerhead sequences is consistent with the idea that k_2 reflects the rate of cleavage chemistry rather than some additional hypothetical step in the kinetic mechanism. If k_2 reflected the rate of a conformational change preceding cleavage, for instance, the rate of a structural transition might be expected to depend on helix sequence and stability. Similar values for k_2 have now been measured for different hammerhead sequences with stabilities calculated (Turner et al., 1988) to range from −6.8 to −13.2 kcal/mol for helix I and from −7.2 to −9.9 kcal/mol for helix III. A structural variant of the hammerhead domain in which the substrate associates with the ribozyme through base pairs in helices I and II, rather than helices I and III, also displayed a cleavage rate on the order of 1 min^{-1} (Uhlenbeck, 1987). Since helix III forms within the substrate in this configuration, the absence of a change in k_2 seems to rule out formation of helix III as the rate-determining step. Furthermore, a large increase in k_2 has been observed between pH 6 and pH 8 (S. C. Dahm and O.C.U., manuscript in preparation), which also supports the idea that k_2 is the rate of cleavage chemistry.

The hammerhead cleavage rate of 1 min^{-1} constitutes a rate enhancement of at least 8 orders of magnitude above the estimated rate of nonenzymatic cleavage of RNA at neutral pH (Shapiro & Vallee, 1989). Hammerhead cleavage is about 4 orders of magnitude slower than RNase A catalysis of the same reaction (Richards & Wycoff, 1971) and about 2 orders of magnitude slower than the *Tetrahymena* ribozyme cleavage reaction that generates 5′-phosphate termini (Herschlag & Cech, 1990). Intermolecular cleavage by the hairpin ribozyme occurs at about the same rate as hammerhead cleavage (Hampel & Tritz, 1989). Because these cleavage rates were not measured under the same conditions, the significance of these comparisons is limited, and it should be noted that the rates reported here for the hammerhead ribozyme pertain to suboptimal conditions of pH, temperature, and $MgCl_2$ concentration. Simultaneous optimization of each of these parameters would likely increase the rate of cleavage by at least an order of magnitude (S. C. Dahm, M.J.F., and O.C.U., unpublished data).

Since substrate and product dissociation were fast with respect to the cleavage rate for hammerhead 8, which has 10 base pairs between the substrate and the ribozyme, K_M' reduces to k_{-1}/k_1 or K_d. Hammerhead 8, therefore, reacts according to a Michaelis–Menten kinetic scheme in which E·S is in equilibrium with E + S during the steady-state phase of a multiple-turnover reaction. When K_M' is equal to K_d, cleavage efficiency, k_{cat}/K_M, will be directly proportional to the affinity between the ribozyme and the substrate. This type of kinetic scheme permits discrimination against substrates that bind poorly, since they will be rejected before cleavage at a faster rate than substrates that bind well.

For substrates that form 12 base pairs with the ribozyme, in contrast, substrate dissociation occurred at a rate on the same order as cleavage chemistry. For hammerheads 13, 13-1, 14, and 15, k_2 values made a significant contribution to K_M' values and these reaction kinetics are better described by the Briggs–Haldane formalism (Briggs & Haldane, 1925). For oligoribonucleotide duplexes, increases in helix stability are reflected primarily in decreased dissociation rates with

relatively little effect on association rates (Porschke & Eigen, 1971; Craig et al., 1971; Porschke et al., 1973; Ravetch et al., 1974). It might be expected that substrates that are slightly larger than those examined here would dissociate at negligible rates relative to cleavage rates. As substrate dissociation rates become small, K_M' values would approach k_2/k_1. Since k_2 values appear to be fixed by the rate of cleavage chemistry and k_1 values are expected to increase only slowly with increasing duplex length, it is possible to calculate a hypothetical lower limit for the hammerhead K_M'. Using a value of 1 min^{-1} for k_2 and a value of 84 μM^{-1} min^{-1} for k_1, the fastest rate constant measured for substrate binding, K_M' values for hammerhead ribozymes are not likely to occur below 10 nM. In other words, when K_d, or k_{-1}/k_1, for a ribozyme–substrate complex is equal to 10 nM, there would be no improvement in K_M' by the formation of additional base pairs between the substrate and the ribozyme. As the stability of the ribozyme–substrate complex increases, the switch from Michaelis–Menten to Briggs–Haldane kinetic mechanisms will reduce the ability of the ribozyme to distinguish among related substrates (Herschlag, 1991). It should be noted that K_M' is not the standard Michaelis–Menten constant which pertains to the steady-state phase of a multiple-turnover reaction. Because substrate selection cannot be altered by events that follow virtually irreversible cleavage, the K_M' value is more important than K_M for evaluating cleavage specificity.

In contrast to the hammerhead ribozyme, the *Tetrahymena* ribozyme binds its substrate with higher affinity (Pyle et al., 1990), and substrate dissociates more slowly (Herschlag & Cech, 1990) than expected for a simple RNA duplex due to hydrogen-bonding interactions between the ribozyme and a 2′-hydroxyl group in the substrate (Pyle et al., 1991). Hammerhead ribozymes that bind substrates through approximately 10 base pairs are expected to cleave with high-specificity Michaelis–Menten kinetics whereas similar substrates are expected to bind the *Tetrahymena* ribozyme with high affinity and to cleave according to a low-specificity Briggs–Haldane kinetic mechanism. Consequently, ribozymes with hammerhead kinetics may be more suited to specific target cleavage in gene inactivation applications.

Substrate binding rate constants varied between 9 and 84 μM^{-1} min^{-1}. These rate constants fall in the range expected for the formation of simple RNA duplexes (Porschke & Eigen, 1971; Craig et al., 1971; Porschke et al., 1973; Ravetch et al., 1974; Breslauer & Bina-Stein, 1977; Nelson & Tinoco, 1982). Low binding rates might be a consequence of the propensity of some RNAs to adopt alternate secondary structures as previously proposed (Fedor & Uhlenbeck, 1990). S13 not only displayed the lowest substrate binding rate constant but also reacted to a lower extent than the other substrates with 30% of the substrate remaining intact after long incubations with ribozyme whereas the other substrates were cleaved nearly to completion (90–95%). The cleavage-resistant fraction of S13 may reflect an alternate secondary structure.

For hammerhead 8, the products bound to the ribozyme by five base pairs, and product release was faster than the rate-determining step of cleavage chemistry (Fedor & Uhlenbeck, 1990). For hammerheads 13, 13-1, 14, and 15, one of the products bound with seven base pairs, and the rate of product dissociation became rate-determining for multiple-turnover reactions with saturating substrate. Dissociation rate constants for small RNA duplexes are directly proportional to the stability of the helix and therefore depend on the number and identity of the interacting nucleotides (Porschke et al., 1973; Ravetch et al., 1974; Breslauer & Bina-Stein, 1977; Nelson & Tinoco, 1982). K_d values and dissociation rates can be estimated for any RNA helix in 1 M NaCl on the basis of data from model experiments (Tinoco et al., 1971; Turner et al., 1988). Calculation of the affinity of S13-P2 for R13 gives satisfactory agreement with measured values. The K_d value of 0.5 nM measured for the R13–S13-P2 complex agrees well with the K_d value of 0.2 nM calculated for the helix. HH13 has a rate of product dissociation 5-fold slower than that of HH14, which contains an G-C to A-U substitution in helix I. This measured difference in product dissociation rate constants agrees well with the 6-fold difference in calculated K_d values for the two helix I sequences. The rapid dissociation rates observed for S13-P1, HH8 products and the P2 product of S13-2 cleavage are also consistent with the calculated stability of these helices. Finally, the stability of the ribozyme–product complex was unaffected by mutations that eliminated catalytic activity, so the affinity of the ribozyme for product was independent of catalytic function. In summary, the equilibrium and kinetic properties of the ribozyme–product complex resembled those expected for a simple RNA duplex with the same sequence.

Comparison of substrate and product dissociation rates shows that products bound in seven base pairs dissociated from the ribozyme more slowly than corresponding substrates that potentially form 12 base pairs with the ribozyme. Whereas product dissociation rate constants and K_d values were similar to those expected for simple RNA duplexes, the stability of the ribozyme–substrate complex was substantially lower than expected. Given the surprising nature of these results, it is important to consider whether alternative explanations could account for the apparent speed of substrate dissociation. Values of k_{-1} were derived from partitioning experiments in which an initial binding period was used to incorporate radioactive substrate into hammerhead complexes whose decay was measured after dilution into chase RNA. If binding of radioactive substrate was incomplete during the brief binding period, a fraction of radioactive substrate would fail to cleave during the subsequent chase although this fraction would have the opportunity to bind and cleave in the parallel reaction without chase RNA. Arguing against this possibility is the fact that the $t_{1/2}$ for binding should be less than 1 s at the concentrations used and the finding that the chased reactions were insensitive to ribozyme concentration and duration of the initial binding period. However, if some fraction of substrate was present in a structure that was unable to bind ribozyme in 20 s but slowly exchanged into reactive conformation over the next few minutes, control reactions would proceed to a greater extent than chase reactions even if substrate dissociation was slow. Such a slowly exchanging alternate conformation might have been detected in experiments to measure substrate dissociation from R13m since any free substrate present after 20 s of binding would be subject to cleavage upon dilution into active ribozyme. However, less than 4% of radioactive S13 was cleaved within 10 min after dilution into active ribozyme in that experiment, arguing that virtually complete binding had occurred. Unless there is a large difference between the kinetics of R13 and R13m binding to substrate, this suggests that the ~15% of S13 uncut at the end of the chase had bound to the ribozyme.

A second explanation for the difference in extent of cleavage between chase and control reactions is that chase RNA might interfere with cleavage by binding the hammerhead complex and interfering with catalysis or accelerating substrate release through a branch migration mechanism. If this were the case, it might be expected that the sequence or concentration of the

chase RNA would affect the propensity to form a ternary complex. However, k_{-1} values for S13 and S13-1 were the same regardless of whether S13, S13-1, S13-2, or S13-P2 was used as chase RNA, and the concentration of chase RNA had no detectable effect on k_{-1} measurements over an 8-fold range.

Perhaps the strongest argument that results of partitioning experiments accurately reflect substrate dissociation rates is the finding that truncations of S13 to generate S13-1 and S13-2 accelerated rates of substrate dissociation by factors that agreed well with corresponding effects on product dissociation rates. Loss of an unpaired nucleotide in S13-1 accelerated the rate of P2 release about 2-fold, and the rate of substrate dissociation appeared to increase almost 1.5-fold. Loss of a base pair between R13 and S13-2 accelerated both product release and substrate dissociation rates so that both became much faster than cleavage chemistry. If apparent k_{-1} measurements were an artifact of incomplete initial binding or ternary complex formation with chase RNA, it is not clear why substrate binding and product dissociation rates should be similarly affected by substrate truncations.

In summary, although the anomalously fast k_{-1} values rest entirely on one type of experiment, we have not found any inconsistency in the data. It will be important to study several other types of hammerheads and to determine k_{-1} values with different methods to confirm this surprising observation.

If E·S is less stable than E·P, substrate binding does not fully exploit all of the stabilizing energy available through base pairing and stacking interactions in the hammerhead helices or interactions between the substrate and ribozyme that do not occur with products contribute positive free energy to E·S. The effect of reduced E·S stability would be to lower the energy barrier between E·S and E·P. This notion is consistent with the theory of enzyme catalysis originally proposed by Haldane (1930) that the active site structure is more complementary to the transition-state structure than to the substrate structure [see recent discussion by Kraut (1988)].

Mutations of catalytically essential nucleotides in the hammerhead core resulted in increased affinity of substrates for the ribozyme without affecting product stability. These ribozyme nucleotides might interact directly with substrate at the active site in a fashion that contributes positive free energy to substrate binding and, perhaps, favors binding to the transition state. Alternatively, these nucleotides might be integral to a catalytically active ribozyme conformation that is incompatible with high-affinity substrate binding, even without direct substrate interactions, in the same way that mutations that disrupt the folded structure of a protein enzyme might eliminate catalysis even if the mutations are at a distance from the active site. Mutation of these nucleotides might stabilize substrate binding by preventing formation of the catalytically active conformation. More information about the structure of hammerhead domain and catalytically inactive hammerhead analogs will help distinguish these possibilities.

Substitution of a deoxyribonucleotide for the ribonucleotide at the cleavage site in the substrate also stabilized substrate binding, although to a lesser extent than ribozyme core mutations. Because the 2′-oxygen is the nucleophile for attack on the phosphate in the transition state, it is clear why elimination of the 2′-hydroxyl prevents catalysis, but this would not necessarily require that the 2′-hydroxyl be involved in substrate binding. Nonetheless, direct steric interference by the 2′-hydroxyl with substrate binding might account for the slightly enhanced affinity for the deoxy-substituted substrate.

The decreased affinity of large substrates compared to smaller products is a surprising result when substrate binding to the hammerhead ribozyme is viewed as annealing of an imperfect duplex. However, an inverse correlation between binding affinity and catalytic activity has ample precedents among protein enzymes. For example, in lysozyme cleavage of *N*-acetylglucosamine oligosaccharides, substrate binding constants increase with substrate size for substrates with one to three sugar residues, but, with more than three residues, the rate of cleavage increases with no increase in binding: a hexameric oligosaccharide cleaves 30 000-fold faster than a trimeric substrate but has a similar binding constant (Rupley & Gates, 1967). Original speculations that steric "strain" accompanied binding of the half-chair or "sofa" conformation required by the carboxonium ion intermediate versus the full chair conformation preferred in solution were not supported by binding experiments (Schindler & Sharon, 1976; Schindler et al., 1977). Computer modeling of the lysozyme active site implicated electrostatic rather than steric strain due to the requirement for the active site to accommodate the carboxonium ion developing in the transition state with consequent loss of optimum "fit" for the uncharged substrate (Warshel & Levitt, 1976). Observations regarding lysozyme substrate binding and catalysis point to the possibility that the source(s) of hammerhead substrate destabilization need not be geometric distortion of the substrate or steric strain but might include electrostatic and desolvation effects.

ACKNOWLEDGMENT

We thank Jamie Williamson, Doug Turner, Dan Herschlag, and Klemens Hertel for helpful discussions, Cheryl Fortier for technical assistance, and David Long, Debbie Diamond, and Ed Scott for critical reading of the manuscript.

REFERENCES

Breslauer, K. J., & Bina-Stein, M. (1977) *Biophys. Chem. 71*, 211–216.
Briggs, G. E., & Haldane, J. B. S. (1925) *Biochem. J. 19*, 338–339.
Buzayan, J. M., Gerlach, W. L., & Breuning, G. (1986) *Proc. Natl. Acad. Sci. U.S.A. 83*, 8859–8862.
Chaix, C., Molko, D., & Teoule, R. (1989) *Tetrahedron Lett. 30*, 71–74.
Craig, M. E., Crothers, D. M., & Doty, P. (1971) *J. Mol. Biol. 62*, 383–401.
Dahm, S. C., & Uhlenbeck, O. C. (1990) *Biochimie 72*, 819–823.
Eadie, G. S. (1942) *J. Mol. Biol. 146*, 85–93.
England, T. E., & Uhlenbeck, O. C. (1978) *Biochemistry 17*, 2069–2076.
Fedor, M. J., & Uhlenbeck, O. C. (1990) *Proc. Natl. Acad. Sci. U.S.A. 87*, 1668–1672.
Fersht, A. R. (1985) *Enzyme Structure and Mechanism*, 2nd ed., pp 143–147, W. H. Freeman & Co., New York.
Forster, A. C., & Symons, R. H. (1987) *Cell 50*, 9–16.
Gold, L., Pribnow, D., Schneider, T., Schinedling, S., Singer, B. D., & Stormo, G. (1981) *Annu. Rev. Microbiol. 35*, 365–403.
Groebe, D. R., & Uhlenbeck, O. C. (1988) *Nucleic Acids Res. 16*, 11725–11735.
Guthrie, C., & Patterson, B. (1988) *Annu. Rev. Genet. 22*, 387–419.
Haldane, J. B. S. (1930) *Enzymes*, pp 180–183, Longmans, London.
Hampel, A., & Tritz, R. (1989) *Biochemistry 28*, 4929–4933.
Haseloff, J., & Gerlach, W. L. (1988) *Nature 334*, 585–591.
Herschlag, D. (1991) *Proc. Natl. Acad. Sci. U.S.A. 88*, 6921–6925.
Herschlag, D., & Cech, T. R. (1990) *Biochemistry 29*, 10159–10171.

Hertel, K. J., Pardi, A., Uhlenbeck, O. C., Koizumi, M., Ohtsuka, E., Uesugi, S., Cedergren, R., Eckstein, F., Gerlach, W. L., Hodgson, R., & Symons, R. H. (1992) *Nucleic Acids Res. 20*, 3252.

Heus, H. A., & Pardi, A. (1990) *J. Mol. Biol. 217*, 113–124.

Heus, H. A., Uhlenbeck, O. C., & Pardi, A. (1990) *Nucleic Acids Res. 18*, 1103–1108.

Hofstee, B. H. J. (1952) *J. Biol. Chem. 199*, 357–364.

Jeffries, A. C., & Symons, R. H. (1989) *Nucleic Acids Res. 17*, 1371–1377.

Keese, P., & Symons, R. H. (1987) in *Viroids and Viroid-like Pathogens* (Semancik, J. S., Ed.) pp 1–47, CRC Press, Boca Raton, FL.

Kochino, Y., Watanabe, S., Harada, F., & Nishimura, S. (1980) *Biochemistry 19*, 2085–2089.

Koizumi, M., Iwai, S., & Ohtsuka, E. (1988a) *FEBS Lett. 228*, 228–230.

Koizumi, M., Iwai, S., & Ohtsuka, E. (1988b) *FEBS Lett. 239*, 285–288.

Koizumi, M., Hayase, Y., Iwai, S., Kamiya, H., Inoue, H., & Ohtsuka, E. (1989) *Nucleic Acids Res. 17*, 7059–7071.

Kraut, J. (1988) *Science 242*, 533–540.

Milligan, J. F., & Uhlenbeck, O. C. (1989) *Methods Enzymol. 180*, 51–62.

Nelson, J. W., & Tinoco, I., Jr. (1982) *Biochemistry 21*, 5289–5295.

Odai, O., Kodama, H., Hiroaki, H., Sakata, T., Tanaka, T., & Uesugi, S. (1990) *Nucleic Acids Res. 18*, 5955–5960.

Pease, A. C., & Wemmer, D. E. (1990) *Biochemistry 29*, 9039–9046.

Perreault, J. P., Wu, T., Cousineau, B., Ogilvie, K. K., & Cedergren, R. (1990) *Nature 344*, 565–567.

Porschke, D., & Eigen, M. (1971) *J. Mol. Biol. 62*, 361–381.

Porschke, D., Uhlenbeck, O. C., & Martin, F. H. (1973) *Biopolymers 12*, 1313–1335.

Prody, G. A., Bakos, J. T., Buzayan, J. M., Schneider, I. R., & Bruening, G. (1986) *Science 231*, 1577–1580.

Pyle, A. M., & Cech, T. R. (1991) *Nature 350*, 628–630.

Pyle, A. M., McSwiggen, J. A., & Cech, T. R. (1990) *Proc. Natl. Acad. Sci. U.S.A. 87*, 8187–8191.

Pyle, A. M., Murphy, F. L., & Cech, T. R. (1992) *Nature 358*, 123–128.

Ravetch, J., Gralla, J., & Crothers, D. M. (1974) *Nucleic Acids Res. 1*, 109–127.

Richards, F. M., & Wycoff, H. W. (1971) in *The Enzymes* (Boyer, P. D., Ed.) pp 647–806, Academic Press, New York.

Rosbash, M., & Seraphin, B. (1991) *Trends Biochem. Sci. 16*, 187–190.

Rose, I. A., O'Connell, E. L., Litwin, S., & Bar Tana, J. (1974) *J. Biol. Chem. 249*, 5163–5168.

Ruffner, D. E., Dahm, S. C., & Uhlenbeck, O. C. (1989) *Gene 82*, 31–41.

Ruffner, D. E., Stormo, G. D., & Uhlenbeck, O. C. (1990) *Biochemistry 29*, 10695–10702.

Rupley, J. A., & Gates, V. (1967) *Proc. Natl. Acad. Sci. U.S.A. 57*, 496–510.

Sampson, J. R., Sullivan, F. X., Behlen, L. S., DiRenzo, A. B., & Uhlenbeck, O. C. (1987) *Cold Spring Harbor Symp. Quant. Biol. 52*, 267–275.

Scaringe, S. A., Francklyn, C., & Usman, N. (1990) *Nucleic Acids Res. 18*, 5433–5441.

Schindler, M., & Sharon, N. (1976) *J. Biol. Chem. 251*, 4330–4335.

Schindler, M., Assef, Y., Sharon, N., & Chipman, D. M. (1977) *Biochemistry 16*, 423–431.

Schultz, J. C., Molko, D., & Teoule, R. (1987) *Nucleic Acids Res. 15*, 397–416.

Shapiro, R., & Vallee, B. L. (1989) *Biochemistry 28*, 7401–7408.

Sheldon, C. C., & Symons, R. H. (1989) *Nucleic Acids Res. 17*, 5679–5685.

Tinoco, I., Jr., Uhlenbeck, O. C., & Levine, M. (1971) *Nature 230*, 362–367.

Turner, D. H., Sugimoto, N., & Freier, S. M. (1988) *Annu. Rev. Biophys. Biophys. 17*, 167–192.

Uhlenbeck, O. C. (1987) *Nature 328*, 596–600.

Usman, N., Ogilvie, K. K., Jiang, M.-Y., & Cedergren, R. J. (1987) *J. Am. Chem. Soc. 109*, 7845–7853.

Warshel, A., & Levitt, M. (1976) *J. Mol. Biol. 103*, 227–249.

Wetmur, J. G., & Davidson, N. (1968) *J. Mol. Biol. 31*, 349–370.